



A study of pyridyl nitrosyl iron(II) tetraphenyl $^{15}\text{N}_4$ -porphyrin. NO geometry and spin coupling to the pyrrole nitrogens

D.C. Gilbert ^a, S.A. Dikanov ^{a,1,2}, D.C. Doetschman ^{a,*}, J.A. Smeija ^b

^a Department of Chemistry, Binghamton University, State University of New York, Binghamton, NY 13902-6016, USA

^b Department of Chemistry, Gonzaga University, Spokane, WA 99258, USA

Received 7 September 1999

Abstract

Spin coupling with pyrrole nitrogens and NO geometry in pyridyl-NO-Fe(II) tetraphenyl- $^{15}\text{N}_4$ -porphyrin, examined with hyperfine sublevel correlation spectroscopy (HYSCORE), was studied because of renewed interest in diatomic molecule bound ferrous hemes, e.g. the physiologically important NO synthase. Dipolar coupling locates the effective electron spin position (0.109 ± 0.008 nm from the ring center, 0.106 ± 0.006 nm above the ring plane and projecting $37 \pm 2^\circ$ from the nearest pyrrole nitrogen). The NO projection in an X-ray study of the 4-methyl piperidine complex is 38.6° . The negative pyrrole nitrogen spin densities induced by the NO obey a sinusoidal angular relationship. © 1999 Elsevier Science B.V. All rights reserved.

1. Introduction

Many electron paramagnetic resonance (EPR), double resonance and electron spin echo envelope modulation (ESEEM) studies have been made of the nitrosylated heme proteins, such as hemoglobin, its isolated subunits, myoglobins and model compounds as spin labeled models of the corresponding oxygenated species [1–11]. Very few of these studies have focused on the pyrrole N couplings because the coupling constants are very small [12]. The small couplings have been unresolvable in continuous wave

(CW) EPR experiments on these systems. The low frequencies required to observe the pyrrole nitrogen electron nuclear double resonance (ENDOR) have also rendered such experiments unsuccessful to date. More successful have been ESEEM studies [12,13]. Nevertheless, randomly oriented samples of nitrosyl hemes and model compounds still pose a challenge to one-dimensional (1D) ESEEM spectroscopies and a recent two-dimensional (2D) HYSCORE [14] study of nitrosylated α and β hemoglobin subunits has achieved significantly better resolution of the ^{14}N resonance frequencies [12].

The ability to understand the structural interactions of the electron spin in nitrosyl heme proteins with surrounding nuclei has assumed renewed importance in recent years. Since the discovery of the biological role and significance of NO [15], interest in the mature subject of nitrosylated hemes has revived. One reason for the revival is that nitrosyl-

* Corresponding author. Fax: +1-607-777-4478; e-mail: ddoetsch@binghamton.edu

¹ Permanent address: Institute of Chemical Kinetics and Combustion, Novosibirsk 630090, Russian Federation.

² Present address: Illinois EPR Research Center, University of Illinois, 506 South Matthews Avenue, Urbana, IL 61801, USA.

tion of hemoglobin occurs physiologically during the induced production of NO due to immune responses, among the most dramatic episodes of which are septic shock and organ transplant rejection [16–18]. Another reason is that research has revealed that NO is synthesized at the site of a P450 type heme protein in the nitric oxide synthase (NOS) enzyme [11,19,20]. Moreover, it has even been shown that NO can bind to this heme, although not necessarily under physiological conditions [11,21]. Finally, there is renewed interest in applying new ESEEM tools, such as the 2D-ESEEM technique, HYSCORE, to the question of cooperativity [5] in nitrosylated hemoglobin. Recent ENDOR studies [7] and a recent ESEEM study [12] indicate that the R and T states of the classical cooperativity hypothesis involve two Fe–(NO) conformations in nitrosyl hemoglobin [6]. A temperature-dependent variation in the spectra of NO-tetraphenyl-porphyrinato-Fe(II) complexes may also be related to this question of conformational variation [8].

For these reasons we undertook a temperature dependence study of the NO-tetraphenyl- $^{15}\text{N}_4$ -TPP-Pyr model compound [8,9] with the HYSCORE method to be presented in this Letter. The ^{15}N nucleus with its larger magnetic moment, with its lower spin $I = 1/2$ and its absence of nuclear quadrupole interaction promised a simpler pyrrole N HYSCORE spectrum with a somewhat wider observability range at X-band fields, based on the relative sizes of the Zeeman and hyperfine interactions [22–24]. A more complete pyrrole ^{15}N study in the model compound would provide a firmer basis for the analysis of the pyrrole ^{14}N compound, a study presently in progress. In turn the ^{14}N model compound study promises to be the stepping stone to the analysis of ESEEM experiments on nitrosylated heme proteins in general, for which pyrrole N isotopic substitution would be a major undertaking.

2. Experimental details

We examined the model compound, NO-tetraphenyl- ^{15}N -porphyrinato-Fe(II)-pyridine (NO-Fe- $^{15}\text{N}_4$ -TPP-Pyr). The compounds were prepared as the five-coordinate nitrosylated species [25–27]. The complex was converted to the six-coordinated pyridyl

form by adding a few drops of N_2 -purged pyridine to a 4 mm EPR tube containing a depth of ~ 2 cm of N_2 -purged 0.5% (w/w) toluene solution of the complex. The EPR tube was degassed and sealed under vacuum. Sample concentrations were ~ 6.2 mM. The samples were flash cooled under liquid nitrogen before insertion into the pre-cooled cryostat.

Four pulse HYSCORE experiments were performed on an X-band Bruker ESP 580 spectrometer with an overcoupled, low- Q , split-ring (optical) resonator. An Oxford CF935 cold-gas-flow cryostat and ITC 502 temperature controller were employed to maintain the sample at temperatures between 15 and 50 K. Frequencies were measured with an internal Bruker frequency counter interfaced to the system. Fields were measured with the calibrated Bruker Hall probe on the magnet face interfaced to the system. A 16-16-24-16 ns microwave pulse sequence with a four-element phase cycle [28] was used with amplitudes adjusted for a maximum 16–24 ns Hahn echo intensity. (The non-ideal pulse sequence was employed to reveal the intra-manifold correlations of the pyridine ^{14}N should it have been observable [29].) The initial pulse interval $\tau = 200$ or 300 ns was chosen to give the maximum ^{15}N modulations. Arrays of 256×256 four-pulse echo intensity points were acquired at 40 ns successive intervals T_1 and T_2 between the last three pulses. Several g -values in the EPR spectra [8] were sampled at each temperature and some weak angular selectivity was observed in the ^{15}N spectra. The arrays were decay baseline corrected, zero-filled to 512×512 arrays, windowed for a smooth transition to the zero-filled region with a Hamming function and fast 2D Fourier transformed from (T_1, T_2) intensity representations to (ν_1, ν_2) representations without phase correction. The absolute value spectra in contour form were used for analysis.

3. Experimental results

Several g -values in the EPR spectra were sampled at each temperature and some weak angular selectivity was observed in the ^{15}N spectra. Fig. 1 shows a typical EPR spectrum together with the g -values at which HYSCORE measurements were made. Ten to twelve data sets at temperatures of 15,

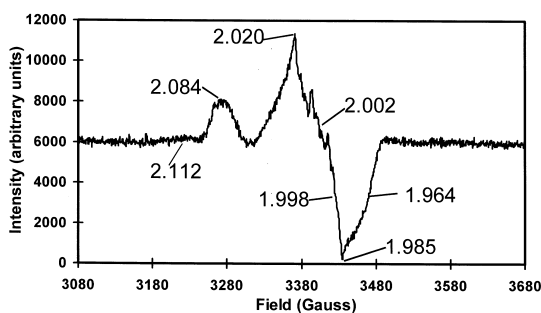


Fig. 1. The 30 K, EPR spectrum of NO-tetra-phenyl- $^{15}\text{N}_4$ -porphyrinato-Fe(II)-pyridine is shown together with the g -values at which HYSCORE measurements were made.

30, 40, and 50 K, were measured at g -value ranges 2.070–2.084, 2.014–2.015, and 1.998–2.002, and at $g = 1.985$. A typical example of the data sets acquired is shown in Fig. 2 along with the assignment of the contour ridges to particular pyrrole nitrogens, obtained from considerations to be discussed in Section 4. The data in Fig. 2, shown up to 5 MHz in two quadrants, are from an experiment at $g = 2.012$ at a temperature $T = 50$ K. Similar data sets were assembled from HYSCORE spectra at various g -values taken at temperatures of 15, 30, and 40 K. No evidence of pyridine ^{14}N correlations were observable in these experiments. Differences observable between the not fully resolved hyperfine structure in

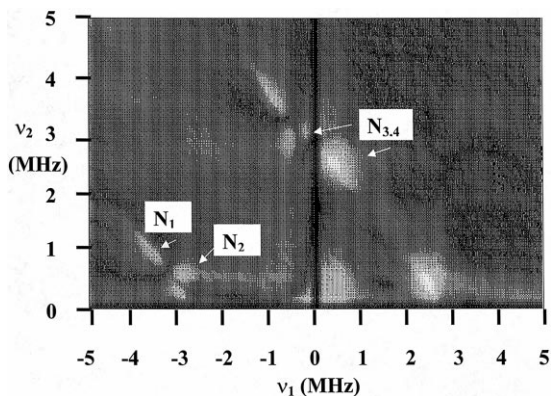


Fig. 2. The 50 K, $g = 2.015$ HYSCORE spectrum of NO-tetra-phenyl- $^{15}\text{N}_4$ -porphyrinato-Fe(II)-pyridine is shown together with the assignment of the correlation features to the pyrrole nitrogens (see numbering in Fig. 4). The intensity scale is a logarithmic gray scale with black and white the lowest and highest intensity, respectively.

the EPR spectra of the ^{15}N - and ^{14}N pyridine substituted compounds suggests that the pyridine N hyperfine coupling is too large to be expected to appear strongly in X-band ESEEM experiments. Experiments over the range of g -values with τ -values chosen to enhance proton resonances revealed no appreciable proton correlation peaks.

4. Analysis of the data

The 50 K example of the two-dimensional data points (ν_1, ν_2) measured along the ridges of the contours of the correlation of $\nu_{\alpha(\beta)}$ with $\nu_{\beta(\alpha)}$ in the NO-Fe- $^{15}\text{N}_4$ -TPP-Pyr spectra, collected at a given temperature and corrected to a common ^{15}N frequency, is shown in Fig. 3 as plots of ν_2^2 vs. ν_1^2 .

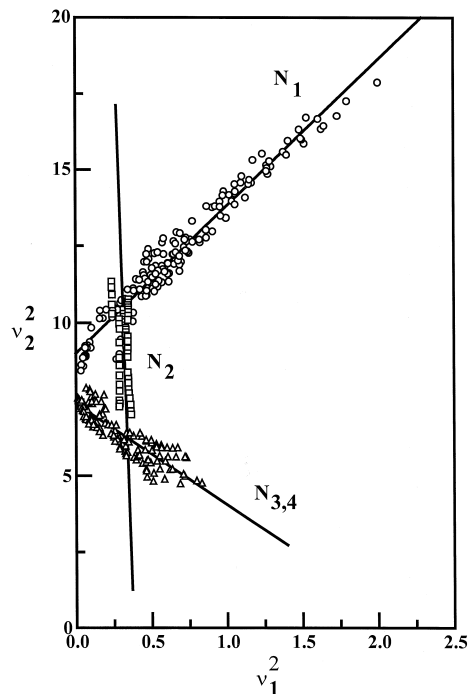


Fig. 3. Plots of the squared correlation frequency coordinates of the contour ridge at 50 K in the HYSCORE spectra of NO-tetra-phenyl- $^{15}\text{N}_4$ -porphyrinato-Fe(II)-pyridine, corrected to a common ^{15}N frequency, are shown. The assignments of the data to the porphyrin pyrrole nitrogens (see definition in caption of Table 1) – N_1 (circle), N_2 (square), and $\text{N}_{3,4}$ (diamond, triangle, respectively) – and the best-fit straight lines for each group of points are also given.

The data were fit by straight lines for each of the three indicated pyrrole ^{15}N observed. The slopes and intercepts of the lines were analyzed according to the method of Dikanov and Bowman [30] for the isotropic and anisotropic hyperfine coupling parameters, assuming a cylindrically symmetric interaction. The parameters obtained at each temperature are presented in Table 1. The uncertainties were determined from the propagation of the calculated errors in the best-fit slopes and intercepts shown in Fig. 3. The ambiguities in the T -values inherent in the numerical solutions using this method were resolved by assuming that the anisotropic part is predominantly of the form predicted by a point dipolar interaction. Thus only the negative T -values are shown in Table 1. The ambiguities in the a values could not be resolved in this study. However, in studies of the ^{14}N model compound in the presence of its non-coaxial quadrupole interaction, it proves to be possible to resolve this ambiguity. These studies indicate that the positive values of $a(^{15}\text{N})$ are the correct values. These values correspond to N 2s orbital electron spin densities of $-0.1903 \times 10^{-2} \pm 0.0015 \times 10^{-2}$, $-0.1297 \times 10^{-2} \pm 0.0008 \times 10^{-2}$, and -0.0857×10^{-2} on N_1 , N_2 , and $\text{N}_{3,4}$, respectively, magnitudes not surprising for atoms not directly involved with bonding or antibonding orbitals of NO to Fe. For

spin densities of this order, a negative spin density is not surprising and not out of line with the observations for vanadyl complexes [31].

Studies of a vanadyl porphyrin complex indicate minor anisotropic dipolar contributions from electron spin density on the pyrrole nitrogens [31]. Therefore we estimated the position of an effective point electron spin from these at 15, 30, 40, and 50 K [6]. A pyrrole ring center to N distance of 0.2007 nm [32] was employed under the assumption of a planar four-fold coordination of equivalent pyrrole nitrogens. See Fig. 4. Least-squares fits of the point spin position to the data under the point dipole approximation gave the positions in Table 2. We do not believe that the apparent variations of the values in Table 2 with temperature are significantly outside uncertainties. The effective, temperature average, point electron spin is located a distance of 0.109 ± 0.008 nm from the porphyrin ring center and 0.106 ± 0.006 nm above the porphyrin ring plane. The temperature average point spin position makes a projection on the porphyrin plane at $37 \pm 2^\circ$ from the nearest pyrrole N_2 , a value in good agreement with the NO bond projection of 38.6° [33]. Only three nitrogens are observed, presumably because the two pyrrole nitrogens farthest from the effective spin (and from the NO group), $\text{N}_{3,4}$ give rise to smaller

Table 1

The anisotropic, T , and isotropic, a , parts of the axial hyperfine coupling matrix A at various temperatures, where $A_{\parallel} = a + 2T$ and $A_{\perp} = a - T$. Standard deviations are given in parentheses. The values were determined from the slopes and intercepts of the best-fit lines in Fig. 2 [30]. The sign ambiguities in the determination were resolved as described in the text. The assignments to the indicated pyrrole nitrogens are described in Section 4. The numbering is shown in Fig. 4

Temperature (K)	Pyrrole nitrogen	T/h (Mhz)	a/h (MHz)
15	N_1	-0.92 (0.03)	5.16 (0.04)
	N_2	-0.81 (0.16)	3.33 (0.06)
	$\text{N}_{3,4}$	-0.52 (0.03)	2.11 (0.03)
30	N_1	-0.88 (0.03)	4.84 (0.04)
	N_2	-0.78 (0.07)	3.29 (0.02)
	$\text{N}_{3,4}$	-0.51 (0.03)	2.18 (0.03)
40	N_1	-0.86 (0.04)	5.05 (0.05)
	N_2	-0.78 (0.07)	3.31 (0.04)
	$\text{N}_{3,4}$	-0.60 (0.03)	1.91 (0.03)
50	N_1	-0.83 (0.03)	4.81 (0.04)
	N_2	-0.76 (0.34)	3.22 (0.14)
	$\text{N}_{3,4}$	-0.64 (0.04)	1.86 (0.06)

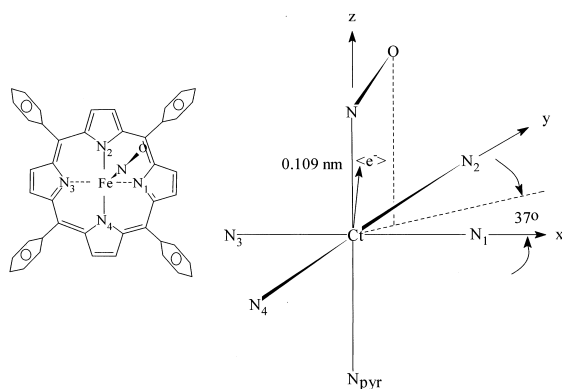


Fig. 4. Model of the NO-tetraphenyl-N-porphyrinato-Fe(II)-pyridine in the vicinity of the pyrrole nitrogens, the Fe and the nitrosyl NO, showing the location of the effective point electron spin in relation to the porphyrin ring center (Ct).

dipolar interactions, leading to their experimental indistinguishability.

The data in Table 1 indicate that there is effectively an inductive effect of the NO projection on the Ns orbital spin density, with the closest, N_2 , exhibiting the a -value with the largest magnitude and the furthest, $N_{3,4}$, exhibiting the smallest value, etc. Accordingly, we fit the empirical relationship in Eq. (1) to the data, where θ is the

$$a(\theta) = a_0 + a_1 \cos(\theta + \delta) \quad (1)$$

angle between a line from the ring center to the respective pyrrole N and the NO projection on the porphyrin ring. The best-fit $a_0/h = 3.50$ MHz, $a_1/h = 1.56$ MHz, and $\delta = 55.5^\circ$ and the root mean square

deviation was $0.14 \text{ MHz} \times h$. Note that these empirical results, which are based on all of the nitrogen a values, predict that N_2 lies 34.5° from the NO projection, a value not far from the value of 37.2° predicted by the point spin model. With this relationship, an environmental perturbation of the nitrosylated porphyrin, such as might be found in a protein environment may be considered. The relationship would apply under circumstances where the Fe–N–O plane is simply rotated about the normal to the ring center, without other changes in geometry resulting in a redistribution of spin relative to the Fe–N–O group. This empirical relationship, together with the point dipole model dipolar interaction, may make it possible to indicate how many pyrrole ^{14}N or ^{15}N would achieve the cancellation condition for maximal ESEEM signal intensity [34,35] at a given NO projection angle on the porphyrin ring plane. Thus the observation of a subset of the pyrrole nitrogens in the HYSCORE spectrum places certain limits on the NO projection or projections consistent with the observation.

5. Summary

A model of the electron spin and the interaction with the pyrrole nitrogens was developed from the analysis of the HYSCORE spectra of the NO-Fe- ^{15}N -TPP-Pyr model compound. The effective center of the electron spin distribution lies ~ 0.106 nm above the porphyrin ring plane, placing it near a

Table 2

Results of the least-squares fit, within the point dipole approximation, of the position (x, y, z) of an effective unit point electron spin to the anisotropic part, $T = -g_e \beta_e g_n \beta_n (x^2 + y^2 + z^2)^{-3/2}$, of the hyperfine coupling constants given in Table 1 at each measurement temperature. Distances $r = (x^2 + y^2 + z^2)^{-1/2}$, from the porphyrin ring center and projection θ of the point spin on the porphyrin plane relative to N_2 are also presented. No individual standard deviations at each temperature were calculated but the temperature average values and standard deviations of the average (in parentheses) are given

T (K)	x (nm)	y (nm)	z (nm)	r (nm)	θ ($^\circ$)
15	0.024	0.020	0.109	0.114	39
30	0.023	0.019	0.113	0.117	39
40	0.014	0.011	0.102	0.103	37
50	0.011	0.007	0.099	0.100	34
Temperature average	0.018 (0.007)	0.014 (0.006)	0.106 (0.006)	0.109 (0.008)	37 (2)

point 62% of the way from the Fe atom to the NO N atom. The projection of the point electron spin on the porphyrin ring plane is in excellent agreement with the NO bond projection on the plane. This is to be expected if one assumes that the effective point electron spin lies in the Fe–N–O plane. The observation of negative spin densities are not surprising for the small magnitudes of the spin densities. An apparent effect of the NO projection over the heme plane is to induce a negative spin density at the pyrrole nitrogens from which an empirical relationship is determined. The relationship restricts the Fe–N–O projections which permit the appearance of strong pyrrole nitrogen resonances.

Acknowledgements

We are grateful for the support of the Chemistry Program of the National Science Foundation under grant no. CHE9512274. Summer research fellowships for D.C.G. from the Department of Chemistry, Binghamton University, and a K. Keith Innes summer research fellowship are gratefully acknowledged.

References

- [1] T. Shiga, K.-J. Hwang, I. Tyuma, *Biochemistry* 8 (1969) 378.
- [2] J.C. Maxwell, W.C. Caughey, *Biochemistry* 15 (1976) 388.
- [3] K. Nagai, H. Hori, S. Yoshida, H. Sakamoto, H. Morimoto, *Biochim. Biophys. Acta* 532 (1978) 17.
- [4] J.F. Deatherage, K. Moffat, *J. Mol. Biol.* 134 (1979) 401.
- [5] S.K. Mun, J.C. Chang, T.P. Das, *Proc. Natl. Acad. Sci. USA* 76 (1979) 4842.
- [6] R.H. Morse, S.I. Chan, *J. Biol. Chem.* 255 (1980) 7876.
- [7] J. Huttermann, C. Burgard, R. Kappl, *J. Chem. Soc., Faraday Trans.* 90 (1994) 3077.
- [8] T. Yoshimura, *Inorg. Chim. Acta* 125 (1986) L27.
- [9] R.S. Magliozzo, J. McCracken, J. Peisach, *Biochemistry* 26 (1987) 7923.
- [10] D.J. Singel, J.R. Lancaster, in: M. Feelisch, J.S. Stamler (Eds.), *Nitric Oxide Research*, Wiley, New York, 1996.
- [11] T. Migita, J.C. Salerno, B.S.S. Masters, P. Martasek, K. McMillan, M. Ikeda-Saito, *Biochemistry* 30 (1997) 10987.
- [12] A.M. Tyryshkin, S.A. Dikanov, E.J. Reijerse, C. Burgard, J. Huttermann, *J. Am. Chem. Soc.* 121 (1999) 3396.
- [13] R.S. Magliozzo, J. Peisach, *Biochemistry* 31 (1992) 189.
- [14] P. Hoefler, A. Grupp, H. Nebenfur, M. Mehring, *Chem. Phys. Lett* 132 (1986) 279.
- [15] M. Feelisch, J.S. Stamler, *Methods in Nitric Oxide Research*, Wiley, New York, 1996.
- [16] J.-C. Drapier, C. Pellat, Y. Henry, *J. Biol. Chem.* 266 (1991) 10162.
- [17] J.R. Lancaster Jr., J.B. Hibbs Jr., *Proc. Natl. Acad. Sci. USA* 87 (1990) 1223.
- [18] J.R. Lancaster Jr., J.M. Langrehr, H.A. Bergonia, N. Murase, R.L. Simmons, R.A. Hoffman, *J. Biol. Chem.* 267 (1992) 10994.
- [19] O.W. Griffith, D.J. Stuehr, *Annu. Rev. Physiol.* 157 (1995) 707.
- [20] B.S.S. Masters, *Annu. Rev. Nutr.* 14 (1994) 131.
- [21] A.R. Hurshman, M.A. Marletta, *Biochemistry* 34 (1995) 5627.
- [22] W.B. Mims, in: S. Geschwind (Ed.), *Electron Paramagnetic Resonance*, ch. 4, Plenum, New York, 1972.
- [23] A.V. Astashkin, S.A. Dikanov, Yu.D. Tsvetkov, *J. Struct. Chem.* 25 (1984) 200.
- [24] H.L. Flanagan, D.J. Singel, *J. Chem. Phys.* 87 (1984) 5606.
- [25] W.R. Scheidt, M.E. Frisse, *J. Am. Chem. Soc.* 97 (1975) 17.
- [26] A.D. Adler, L. Sklar, F.R. Longo, J.D. Finarelli, M.G. Finarelli, *J. Heterocycl. Chem.* 5 (1968) 669.
- [27] R.A.W. Johnstone, M.L.P.G. Nunes, M.M. Pereira, A.M. d'A. Rocha Gonsalves, A.C. Serra, *Heterocycles* 43 (1996) 1423.
- [28] C. Gemperle, G. Aebli, A. Schweiger, R.R. Ernst, *J. Magn. Reson.* 88 (1990) 241.
- [29] R. Szosenfogel, D. Goldfarb, *Mol. Phys.* 95 (1998) 1295.
- [30] S.A. Dikanov, M.K. Bowman, *J. Magn. Reson. A* 116 (1995) 125.
- [31] K. Fukui, H. Ohya-Nishguchi, H. Kamada, *Inorg. Chem.* 24 (1997) 5518.
- [32] P.L. Piciulo, G. Rupprecht, W.R. Scheidt, *J. Am. Chem. Soc.* 96 (1974) 5293.
- [33] W.R. Scheidt, A.C. Brinegar, E.B. Ferro, F.J. Kirnek, *J. Am. Chem. Soc.* 99 (1977) 7315.
- [34] A.V. Astashkin, S.A. Dikanov, Yu.D. Tsvetkov, *J. Struct. Chem.* 25 (1984) 200.
- [35] H.L. Flanagan, D.J. Singel, *J. Chem. Phys.* 87 (1984) 5606.